Published in final edited form as:

Nature. 2014 April 17; 508(7496): 411–415. doi:10.1038/nature13069.

miRNAs trigger widespread epigenetically-activated siRNAs from transposons in *Arabidopsis*

K.M. Creasey[1], **J Zhai**[2], **F. Borges**[1], **F. Van Ex**[1], **M. Regulski**[1], **B.C. Meyers**[2], and **R.A. Martienssen**[1],[3],[4]

[1]Cold Spring Harbor Laboratory, 1 Bungtown Road, Cold Spring Harbor, NY 11724

[2]15 Innovation Way, University of Delaware, Newark, DE 19711

[3]HHMI-GBMF Investigator in Plant Biology, Cold Spring Harbor Laboratory

[4]Chaire Blaise Pascal, Institut de Biologie de l'Ecole Normale Supérieure (IBENS), 75230 Paris France

Abstract

In plants, post-transcriptional gene silencing (PTGS) is mediated by DICER-LIKE1 (*DCL1*)-dependent miRNAs, that also trigger 21-nt secondary siRNA via RNA DEPENDENT RNA POLYMERASE6 (RDR6), DCL4, and ARGONAUTE1 (AGO1)[1–3], while transcriptional gene silencing (TGS) of transposons is mediated by 24-nt heterochromatic (het)siRNA *RDR2*, *DCL3* and *AGO4*[4]. Transposons can also give rise to abundant 21-nt "epigenetically activated" small interfering RNAs (easiRNAs) in *DECREASE IN DNA METHYLATION1* (*ddm1*) and *DNA METHYLTRANSFERASE1 (met1*) mutants, as well as in the vegetative nucleus of pollen grains[5], and in dedifferentiated plant cell cultures[6]. Here we show that easiRNAs resemble secondary siRNAs, in that thousands of transposon transcripts are specifically targeted by more than fifty miRNAs for cleavage and processing by *RDR6*. Loss of *RDR6*, *DCL4* or *DCL1* in a *ddm1* background results in loss of 21-nt easiRNA, and severe infertility, but 24-nt hetsiRNA are partially restored, supporting an antagonistic relationship between PTGS and TGS. Thus miRNA-directed easiRNA biogenesis is a latent mechanism that specifically targets transposon transcripts, but only when they are epigenetically reactivated during reprogramming of the germline. This ancient recognition mechanism may have been retained both by transposons to evade long-term heterochromatic silencing, and by their hosts for genome defence.

For correspondence, R. A. Martienssen (martiens@cshl.edu).

Author Contributions

R.M., B.M. and K.C. designed study. F.B., M.R. and K.C. performed experiments. J.Z. and K.C. analyzed data. R.M. and K.C. prepared manuscript.

Endnotes

Gene Expression Omnibus
GSE52952
GSE52067
GSE52342
GSE52346
GSE52951

21-nt sRNAs, that we have termed easiRNAs, were previously found to accumulate from the 3′ UTR of *ATHILA6* retrotransposons in wild type pollen and *ddm1* inflorescence[5], and to depend on *RDR6, DCL4* and *AGO1*[7,8]. To assess the origin of easiRNAs, we performed small RNA sequencing from inflorescence tissue, and we found that they accumulated in *ddm1*, but not in WT (Columbia-0) nor in *ddm1 rdr6* double mutants[7,8] (Fig. 1; Extended Data Fig. 1a). 21-nt easiRNAs in *ddm1* mostly originated from *ATGYPSY* LTR retroelements (Supplementary Table 1) located in pericentromeric regions, especially the high copy but defective *ATHILA* retrotransposons, which are integrated into pericentromeric satellite repeats (Fig. 1). However, easiRNAs also arose from *ATCOPIA* families found in euchromatic regions, such as *EVADE/ATCOPIA93*[9] (Supplementary Table 1), and from specific *VANDAL/MuDR, HAT* and *CACTA* elements (such as *AtEnSpm6*), some of which are present in much lower copy number and known to transpose in *ddm1*[10]. This raised the important question as to how specificity was conferred to these TEs such that they gave rise to easiRNA, when other transposons and genes did not. Genetically, easiRNA resemble 21-nt *trans*-acting (ta)siRNAs and other secondary siRNA, which are derived from non-coding RNA and mRNA respectively, and are triggered by miRNA bound by *AGO7*[11] and *AGO1*[2,3,12,13]. miRNA were thus excellent candidates to confer transposon specificity.

miRNA biogenesis in *Arabidopsis* depends largely on *DCL1*, so that miRNA are greatly reduced in sterile *dcl1-9*, and partly reduced in fertile *dcl1-11*[14]. We were unable to recover *ddm1 dcl1*-9 double mutants, but easiRNA levels were reduced in *ddm1 dcl1-11*, consistent with a role for miRNA in targeting and easiRNA biogenesis (Fig. 1; Extended Data Fig. 1b). We identified miRNAs in our sRNA sequencing libraries from Col-0, *ddm1* and *ddm1 rdr6* inflorescence tissue. In addition to utilising a miRNA identification algorithm[15], miRNAs were distinguishable from other 21-nt sRNAs that are *RDR6*-dependent, by comparing their abundance in *ddm1* and *ddm1 rdr6*. We identified several known miRNAs, validating our algorithm (Extended Data Fig. 10; Supplementary Table 2) and genome-wide target prediction revealed that 3662 TEs are potentially targeted by these miRNAs (Supplementary Table 3). To determine whether miRNAs mediate targeting and cleavage of TE transcripts, we sequenced cleavage sites genome wide by Parallel Analysis of RNA Ends (PARE)[11]. In order to assess specificity, 5′ RNA ends from a 5-nt (s) window surrounding each predicted miRNA target site were compared to those from a larger 30-nt (l) window (Supplementary Table 3; for more specific 1-nt (ss) and 3-nt (sl) windows, refer to Supplementary Table 9). Significant enrichment of RNA ends at or near the target site was strong evidence for cleavage of the transposon transcripts guided by miRNA.

Approximately half of the 3662 predicted TE targets showed evidence of miRNA guided cleavage (Supplementary Table 3), and were targeted by more than fifty distinct miRNA (Extended Data Fig. 10), although some TEs had only one cleavage product in the target window (such as *EVADE/ATCOPIA93*, which is predicted to be cleaved by miR833). In some cases multiple miRNAs targeted single TEs (Extended Data Fig. 10), reminiscent of the “two-hit” model for tasiRNA biogenesis[16]. In other cases, TEs were targeted by longer forms of miRNA (22-nt), which are thought to promote secondary siRNA biogenesis[3,17]. Specifically, 1733 TE were predicted to be miRNA targets and generated easiRNAs (at least 10 reads). Of these, 1247 were detectably cleaved by PARE-seq. An additional 1929 TEs

were predicted to be targeted by miRNAs but, did not generate easiRNAs, of these 442 were detectably cleaved by PARE-seq. Thus, more than half of the TEs targeted by miRNA also generated easiRNA in inflorescence tissue from *ddm1*. However, phasing of easiRNA, typical of other secondary siRNA, was not detected, likely due to the repetitive nature of the TE targets and their targeting by multiple miRNA (data not shown).

Interestingly, the miRNAs found to target TEs, were mostly known miRNAs (Extended Data Fig. 10), such as miR156, miR159, miR172 and miR859, which also generate secondary siRNAs from mRNA targets[2,3]. Many of these miRNAs were predicted to target *ATHILA* elements (Extended Data Fig. 1), generating abundant easiRNA corresponding to *ATHILA ORF1*, also known as *TRANSCRIPTIONALLY SILENT INFORMATION* (*TSI*) (Fig. 2a). *ATHILA ORF1* contains a predicted target site for miR859, and PARE confirmed cleavage at this site (Fig. 2c, Supplementary Table 3). We further validated miR859-directed cleavage by modified 5′ RLM RACE PCR (Fig. 2e).

Despite cleavage of many TE families by multiple miRNAs (Extended Data Fig. 1), some did not generate easiRNAs. This was especially true of *CACTA* and *ATCOPIA* elements, for which most cleavage events were non-productive. For example, *ATCOPIA43* elements were targeted by miR390, which targets non-coding RNA for tasiRNA production by the two-hit model[16], but which did not generate easiRNAs in *ddm1* (Fig. 2b). Instead, PARE detected uncapped degradation products from *ATCOPIA43* indicating extensive secondary RNA decay (Fig. 2d), following miRNA cleavage (Fig. 2f), and similar mRNA decay patterns were found at many genes targeted by miRNA (Extended Data Fig. 2). In general, easiRNA-producing TEs were intact *AtEnSpm2*, *AtEnSpm5*, *AtEnSpm6*, *ATCOPIA93* and *ATCOPIA28* elements, while those that did not generate easiRNAs were non-autonomous elements (e.g. *AtEnSpm1A*), interrupted by insertion of other TEs, or otherwise truncated, and were subject to RNA decay. Occasionally, TEs were found to produce easiRNAs, and were predicted to be targeted by miRNAs, but cleavage could not be detected by PARE, which may be due to the underrepresentation of some miRNAs in inflorescence tissue (Supplementary Table 2). For example, *EVADE/ATCOPIA93* produces abundant easiRNAs from the *GAG* gene, which is predicted to be targeted by several known miRNAs and eamiRNAs (Extended Data Fig. 3a), yet only miR833 shows evidence of cleavage by PARE, and this did not pass our cut-off for miRNA cleavage (Supplementary Table 3). *EVADE/ATCOPIA93* is specifically expressed in only a subset of cells[18].

Two new classes of miRNAs were found in *ddm1*, namely those encoded by transposons, and those miRNA precursors silenced by DNA methylation. We have assigned these miRNAs as epigenetically-activated (ea)miRNAs, as alike easiRNAs, they are abundant in pollen and *ddm1* (Extended Data Fig. 4; Extended Data Fig. 10; Supplementary Table 2). We also identified new miRNA isomers, from 21-nt to 22-nt and 24-nt sequence variants, originating from known miRNA precursors (Supplementary Table 2). 22-nt isoforms promote secondary siRNA biogenesis[3,17] while 24-nt isoforms promote DNA methylation[9,19]. The newly identified eamiR2, originates from an immature precursor sequence within an *ATHILA4* retroelement and is abundant in *ddm1* only (Supplementary Table 2). PARE analysis of *ddm1* confirmed release of this eamiRNA from its own *ATHILA4* precursor (Supplementary Table 3), and cleavage of other *ATHILA4* elements *in*

trans (Fig. 1). However, this TE-derived eamiRNA does not appear to direct easiRNA biogenesis from its own precursor (Supplementary Table 1). Thus, the release of TE-producing eamiRNAs by DICER does not trigger easiRNA biogenesis *per se*, but only when the miRNA targets TE transcripts via AGO1[7].

In order to test the requirement for miRNA in easiRNA biogenesis, we utilized miR845b, a 22-nt miRNA predicted to target several retroelements (Supplementary Table 3), but only in pollen where it is specifically expressed. We fused a GFP reporter gene to a ubiquitously expressed promoter, and to a 300 bp region of *AtGP1* that included the predicted miR845b target site (Fig. 3a). Sequencing small RNA from pollen revealed novel 21-nt easiRNAs surrounding the miR845b target site (Fig. 3a) not found in constructs in which the target site was deleted (Fig. 3b). We confirmed by modified 5′ RNA Ligation-Mediated (RLM) RACE PCR that miR845b-directed cleavage products from *GFP-AtGP1* transcripts accumulate exclusively in pollen (Fig. 3c). Thus, 21-nt easiRNA biogenesis at TEs depends on targeting by miRNA.

24-nt hetsiRNAs guide asymmetric CHH methylation at TEs and are *RDR2*-dependent[4]. We profiled 24-nt hetsiRNAs in Col-0, *ddm1*, *rdr6*, *ddm1 rdr6*, and *ddm1 dcl1-11* (Supplementary Table 1; Fig. 4). In Col-0, 24-nt hetsiRNAs target LTR retrotransposons, and most DNA transposons (Extended Data Fig. 5). In *ddm1*, we found a slight increase of multiple mapping 24-nt hetsiRNAs from *ATGYPSY* retrotransposons that were saturated by easiRNA biogenesis (Supplementary Table 1), but an overall general loss from DNA transposons and other individual retrotransposons, so that less than half of these retained 24-nt siRNA in *ddm1* (Extended Data Fig. 5). Many of these TEs gained 24-nt hetsiRNAs in *ddm1 rdr6* and *ddm1 dcl1* (Supplementary Table 1; Extended Data Fig. 5) and, furthermore, hundreds of TEs that did not have detectable hetsiRNAs in Col-0 or *ddm1*, gained them in *ddm1 rdr6* (Fig. 4a; Extended Data Fig. 6). We hypothesized that miRNA targeting and easiRNA biogenesis might inhibit 24-nt hetsiRNA production in *ddm1*, and we found that almost all TEs cleaved by miRNA either gained 21-nt easiRNAs in *ddm1*, lost 24-nt hetsiRNA in *ddm1*, or gained 24-nt hetsiRNA in *ddm1 rdr6* (Fig. 4b, c; Extended Data Fig. 6). This enrichment was even greater for those TEs targeted by more than one miRNA (Extended Data Fig. 6c).

Thus miRNA cleavage appears to inhibit 24-nt siRNA biogenesis in a manner that depends on RDR6, whether or not easiRNA accumulate (Fig. 4b; Supplementary Table 3). This response was observed when miRNA cleavage sites were on the antisense or occasionally on the sense (mRNA) strand (Supplementary Table 3). It is possible, therefore, that miRNA-directed cleavage of antisense Pol IV/Pol V transcripts, and processing by *RDR6* rather than *RDR2*, might prevent the formation of 24-nt siRNAs, without necessarily generating 21-nt easiRNAs (that are Pol II dependent[8]). Thus, *RDR6* partially antagonizes *RDR2* activity, inhibiting 24-nt hetsiRNA biogenesis at TEs. Likewise, *RDR2* partially antagonizes *RDR6* activity at transgenes subject to PTGS[20].

Symmetric CG and CHG methylation contexts are maintained by DNA methyltransferases and histone modifications, while CHH methylation is associated with 24-nt hetsiRNA guided RdDM[4]. Methylation mediates transcriptional silencing of TE promoters[21], found

near the TIR of most DNA transposons and in the LTR of retrotransposons, as well as internally in the case of the *ATHILA ORF1* and some DNA transposons. As expected, whole-genome sequencing of bisulphite-treated DNA from inflorescence tissue showed global loss of DNA methylation from all classes of transposons in *ddm1* when compared to wildtype, Col-0 (Extended Data Fig. 7a, b). As previously reported, most of this loss occurred in the symmetric CG and CHG contexts, rather than the asymmetric CHH context, consistent with retention of 24-nt hetsiRNA (Supplementary Table 4)[22]. By whole genome bisulphite sequencing we measured levels of DNA methylation in *ddm1 rdr6* F3 progeny from two independent double mutants, relative to *ddm1* (Extended Data Fig. 7a). A modest difference in DNA methylation is expected due to inbreeding of the *ddm1* parents[23], and was observed in one *ddm1 rdr6* replicate, however, methylation at TEs substantially increased in the other replicate (Extended Data Fig. 7e, f; Supplementary Table 4). These results suggest that elevated levels of 24-nt siRNA could only guide remethylation of TEs stochastically in *ddm1 rdr6* (Extended Data Fig. 7g, h), likely reflecting the epigenetic inheritance of unmethylated and methylated TEs from the *ddm1* and *rdr6* parents, respectively, as previously observed[24].

In order to assess whether the loss of the easiRNA pathway leads to a further outburst of transposon reactivation in *ddm1 rdr6*, we utilized Affymetrix *ATH1* microarrays to analyse the transcriptome. A few hundred representative TEs are included on Affymetrix *ATH1* microarrays, and can be used to assess TE reactivation[5]. We found that most of these TE transcripts were abundantly and similarly expressed in both *ddm1* and *ddm1 rdr6* (Supplementary Table 5; Extended Data Fig. 8), indicating that easiRNA biogenesis does not reduce TE transcript levels in *ddm1*. In fact, consistent with our findings of sporadic TE methylation and gain of hetsiRNAs in *ddm1 rdr6*, several TEs had reduced expression in *ddm1 rdr6*, including *ATHILA* and *ATCOPIA* elements, as well as TEs of the MuDR Superfamily (Supplementary Table 5). Therefore, the loss of both *DDM1* and *RDR6* does not enhance transcriptional reactivation of TEs, but instead, some TEs become transcriptionally repressed in *ddm1 rdr6* (Extended Data Fig. 8; Supplementary Table 5), and elevation in methylation level is observed at least for some of these TEs, for example, *ATCOPIA22* and *ARNOLD3*, in *ddm1 rdr6* (Supplementary Table 4).

We have found that loss of TE methylation results in epigenetic activation and consequent transcription, whereby transposon mRNA become preferentially targeted by more than 50 miRNAs bound to *AGO1*. Productive cleavage of transposon transcripts usually engages *RDR6*, allowing *DCL4* to generate 21-nt epigenetically-activated (ea)siRNAs from transposon open reading frames, in a PTGS mechanism (Extended Data Fig. 9). About half of these transposons belong to the LTR/*ATHILA* element family (Extended Data Fig. 10), which occur in high copy number at pericentromeric repeats, and are targeted by multiple miRNAs (Extended Data Fig. 3c; Fig. 2). Several known MIRNA genes, for example miR843, are methylated, and only target transposon transcripts when unmethylated and expressed: in pollen, and in *ddm1* mutants (Supplementary Table 2; Extended Data Fig. 4). Other miRNAs are developmentally regulated, for example miR156, which is required to maintain the juvenile phase of plant development, and miR172, which is required for the

transition to the adult phase[25], accounting perhaps for tissue-specific silencing of TEs during different phases of plant development[26–28].

TEs are targeted by the same conserved miRNA (miR845) in rice and *Arabidopsis* leading to the idea that they may have retained miRNA-binding sites despite selection against them. Furthermore, some of the newly identified miRNAs are themselves encoded by TEs (Extended Data Fig. 10). Why would transposons retain miRNA sites that could potentially silence them post-transcriptionally? One explanation lies in the preferential processing of targeted TE transcripts via *RDR6*, that appears to act antagonistically to *RDR2*, preventing 24-nt hetsiRNA biogenesis (Extended Data Fig. 9)[20]. We found a striking overlap between TEs that produced easiRNAs in *ddm1*, with those that gain 24-nt hetsiRNAs in *ddm1 rdr6* (Fig. 4b, Extended Data Fig. 6). 24-nt hetsiRNA promote RNA dependent DNA methylation (RdDM), and it is likely, therefore, that TEs tolerate developmentally regulated PTGS by miRNA and easiRNAs to avoid long-term TGS by DNA methylation. Given the likely evolution of miRNA precursors from TEs and other inverted repeats[21], miRNAs may have arisen in ancient eukaryotes to target retrotransposons and other TEs rather than genes.

ddm1 mutants are remarkably normal, despite the heritable loss of heterochromatin. In contrast, *ddm1 rdr6*, *ddm1 dcl4* and *ddm1 dcl1* have a wide range of developmental phenotypes and heritable epigenetic defects, including widespread infertility in subsequent generations (K.M. Creasey and R.A. Martienssen, unpublished data). We, therefore, postulate that the function of easiRNAs for the host is to protect the genome from TE-mediated epigenomic instability via PTGS. Consistent with this idea, easiRNAs specifically target the *ATHILA ORF1* gene[29], thought to be involved in retrovirus-like particle formation, as well as the *ATCOPIA* integrase gene and the *CACTA* transposase gene, required for transposition (Extended Data Fig. 3b; Fig. 4c). *RDR6*-directed PTGS could be dangerous to the host by presenting an opportunity to the TE for evasion and transposition, while *RDR2*-directed TGS is a safer silencing strategy not requiring transcription. An important developmental stage during which PTGS is deployed is in the pollen grain, when pericentromeric retrotransposons, and some DNA transposons, lose CHH methylation and RdDM in the male germline[30]. Many of these same TEs accumulate easiRNAs in sperm, which are generated by TE activation in the companion vegetative nucleus, accompanied by the loss of DDM1[5]. Transient loss of RdDM in sperm is restored after fertilization by maternal 24-nt hetsiRNAs[30,31] allowing an opportunity to distinguish “self” from “non-self” pollen upon fertilization, according to whether the transposon load is sufficiently foreign not to be recognized by maternal small RNAs. PTGS, mediated by easiRNAs, would provide a backup silencing mechanism during this critical but potentially dangerous window. A similar secondary siRNA transposon control mechanism, triggered by piRNA rather than miRNA, has recently been described in *C. elegans* and may have similar roles[32,33].

Supplementary Methods

Biological Plant Materials, DNA and RNA isolation

Genomic DNA and Total RNA were isolated from inflorescence tissue collected from Columbia-0 wildtype (WT) and loss of function lines in *ddm1-2*, *rdr6-15*, *ddm1-2 rdr6-15*, and *ddm1-2 dcl1-11* in a Columbia-0 background, grown under standard long-day growth

conditions. The *ddm1-2* line used in this study was in the fifth generation of inbreeding and used for the genetic cross *rdr6-15.* Double heterozygous lines were selected, selfed and second generation *ddm1-2 rdr6-15* were isolated for sequencing in this study. DNA was isolated from pooled inflorescence tissue (n = 3) collected phenol/chloroform extraction. Total RNA was isolated from pooled inflorescence tissue (n = 3) and TRIzol (Invitrogen) extraction following manufacturers instructions.

Small RNA Sequencing Library Construction and Analysis

Pooled inflorescence tissue between stage 9 and 11 (unopened/just opened flowers) (n = 3). Col-0, *ddm1-2, rdr6-15* and *ddm1-2 rdr6-15* TruSeq small RNA sequencing libraries, sequenced on Illumina HiSeq. For the Col-0, *ddm1-2* replicates, and *ddm1-2 dcl1-11* small RNA sequencing libraries were prepared by NEBNext multiplex small RNA libraries, sequenced on Illumina MiSeq. Mapping sRNA-Seq was performed using Bowtie from the open-source Tuxedo suite, allowing for both unique (U) and multiple (M) mapping reads, normalized by reads per million (RPM). Library read count given in Supplementary Table 1.

Whole-Genome Bisulphite Sequencing Library Construction and Analysis

Library construction and bisulphite conversion were carried out, essentially, as described in[34]. For each library, 1–5 μg of genomic DNA was sheared using a Covaris S220 Adaptive Focused Acoustics ultra sonicator. Libraries were constructed following standard protocol using the NEB Next DNA Sample Prep Master Mix Set 1 (NEB E6040) and Illumina-compatible paired-end adaptors, which had all cytosines, methylated. 50 ng of each library was treated with sodium bisulphite using EZ DNA Methylation-Gold™ Kit (Zymo Research D5005) according to the protocol provided by the manufacturer. For each purified library 5–10 ng of purified library was amplified using Expand High Fidelity PLUS PCR system (Roche 03300242001), which is capable of efficiently amplifying uracil-containing templates. 50 μl reactions contained 200 μM each dNTP, 1 μM primer, 2.5 mM $MgCl_2$ and 2.5 U Expand HiFi enzyme, and were performed according to the manufacturer's instructions for 18 cycles. Amplified libraries were ran on 2% MetaPhor® agarose (Lonza 50108) gel. Fragments of 220–350 bp were excised from gel and purified using the QIAquick PCR Purification kit (Qiagen 28104). DNA concentrations were quantified on Bioanalyzer (Agilent), diluted to 10 nM and loaded on flow cells to generate clusters. Libraries were sequenced on Illumina GAII or HiSeq2000 machines using the paired-end 50 cycles protocol. Mapping of BIS-seq libraries performed utilizing Bismark[35]. Library read count given in Supplementary Table 8. For statistical analysis of TE methylation in *ddm1 rdr6* replicates compared to *ddm1*, we performed Binomial Exact Test, alternative = two-sided, taking the total methylation per transposon superfamily and asking the number of TEs that are more methylated in *ddm1 rdr6* compared to *ddm1*, and the number of TEs less methylated, p-value < 2.2e-16 alternative hypothesis: true probability of success is not equal to 0.5, 95 % confidence interval, sample estimates: probability of success given (Supplementary Table 10).

miRNA Identification

Our miRNA prediction algorithm[36] was utilized to identify miRNAs. In total, 128 precursors were identified, representing 96 unique miRNA candidates. Among these 96 sequences, 50 were annotated as *Ath* miRNA in miRBase v17. Abundances of these sequences are shown Supplementary Table 2. t/r/sn/snoRNA related reads were filtered and the miRNA abundance to be at least 10 (normalized abundance) in one or more libraries and with genome hits no more than 20. The sRNAs passed this filter were mapped to the genome and precursor structure was checked by miREAP, developed by BGI, http://sourceforge.net/projects/mireap/). Each precursor was defined by extending from the abundant tag (as potential miRNA) on either side, up to 200-nt to the potential miRNA-star site. After this, two additional filters (strand bias and top1 + top2 ratio) were applied to distinguish miRNA from siRNA loci. Strand bias was calculated by the sum of sRNA abundance on sense strand divided by the total abundance on both strands. Top1 + top2 is the proportion of the abundance of top2 abundant tags, also referred as distribution filter. The cut-off applied was based on known miRNAs from *Ath* and *Osa*. The number of known *Ath*-miRNAs remaining served as an indicator of the efficiency of the filtering. CentroidFold was used with default settings to visualize the overall miRNA precursor structure for manual evaluation. miRNA target prediction was performed using the Noble sRNA targeting resource http://plantgrn.noble.org/psRNATarget/.

Whole Genome PARE-Sequencing Library Construction and Analysis

mRNA purification using Invitrogen Dynabeads mRNA purification kit. 5′ Adaptor ligation. Reverses Transcription for PARE following first strand cDNA synthesis, (short PCR) 7 cycles, (long PCR) 35 cycles. cDNA purification by AMPure XP. Ligation of 3′ double-stranded DNA adaptor overnight. PCR amplification of PARE library (long PCR) 15 cycles followed by PAGE purification. 5′-PARE RNA adaptor 5′-GUUCAGAGUUCUACAGUCCGAC-3′. Target RT-primer: 5′ CGA GCA CAG AAT TAA TAC GAC TTT TTT TTT TTT TTT TTT. Short PCR primer: 5′-adapter primer 5′-GTTCAGAGTTCTACAGTCCGAC-3′ 3′-adapter primer 5′-CGAGCACAGAATTAATACGACT-3′ dsDNA adapter (PARE TruSeq Duplex) (PAGE purified): dsDNA_2_Top: 5′-TGG AAT TCT CGG GTG CCA AGG dsDNA_2_Bottom: (5′Phos) 5′-CCT TGG CAC CCG AGA ATT CCA NN Final PCR primer (P2 sRNA long primer) 5′: AATGATACGGCGACCACCGACAGGTTCAGAGTTCTACAGTCCGA. Indexed Truseq 3′sRNA primer, Index 1~24.

PARE-Sequencing analysis performed by defining two flanking windows at each predicted target site. The sum of abundance of PARE tags matching to (1) a small window (W_S) of 5-nt (cleavage site ± 2-nt), and (2) a long window (W_L) of 31-nt (cleavage site ±15 nt) was calculated. Cleavage sites were filtered to retain those for which $W_S/W_L \geq 0.5$ in the PARE-seq libraries; sites failing this criteria were considered background mRNA cleavage levels. Some chloroplast contamination can account for the distribution of raw read count abundances in our libraries. However, when comparing to the normalization basis, and the mapping of PARE-tags to multiple loci, these reads appear to be of chloroplast mRNA in origin.

The miRNA target lists were filtered by combining both miRNA target penalty score (≤ 7) with PARE-seq data filters of $W_S/W_L \geq 0.3$ and $W_S \geq 3$ (strict), or relaxed; miRNA target penalty score (≤ 7) with PARE-seq data filters of $W_S/W \geq 0.3$ and $W_S \geq 2$. Library information given in Supplementary Table 8. For statistical significance we performed the Chi-square Goodness of Fit Test, calculating the p-value for observed value given the expected value. If we assume PARE tags fall randomly on all the positions in the long window (31-nt), the expected frequency for PARE reads fall into the small window (5-nt) would be 5/31, therefore, the expected frequency would be would 26/31 for other regions. *AtGRF8*, target of miR396, in Col-0, we observe 603 in the small window, and, 614 in the long window (614 − 603 = 11 in other region), the Chi-squared test for given probabilities c(603, 11) X-squared = 3057.857, df = 1, p-value < 2.2e-16 (Supplementary Table 3). For specific miRNA targeting, the sum of abundance of PARE tags matching to (1) a shorter small window (W_{Ss}) of 1-nt (cleavage site ± 0-nt), and (2) a shorter long window (Ws_L) of 3-nt (cleavage site ±1nt) was calculated (Supplementary Table 9).

5′ RLM RACE-PCR

As per instructions 5′ RLM-RACE mapping the cleavage of miRNA FirstChoice (Ambion). 5′ RLM-RACE Adapter ligation followed by RT-PCR, followed by two PCRs (outer and inner), cloning and sequencing. 5′ RLM-RACE adapter: 5′-GCUGAUGGCGAUGAAUGAACACUGCGUUUGCUGGCUUUGAUGAAA-3′. 5′ RLM-RACE outer primer: 5′-GCTGATGGCGATGAATGAACACTG-3′. 5′ RLM- RACE inner primer: 5′-CGCGGATCCGAACACTGCGTTTGCTGGCTTTGATG-3′.

Supplementary Material

Refer to Web version on PubMed Central for supplementary material.

Acknowledgments

We thank Vincent Colot, Oiliver Voinnet and Alexis Sarazin for sharing unpublished data and for discussions, Joseph Simorowski for plant genetics, and Jude Kendall for computational advice. We thank Keith Slotkin for sharing data before publication. K.C. and M. R. were supported, in part, by a research collaboration with DuPont Pioneer. F.V. was supported by a fellowship from the Belgian American Educational Foundation (B.A.E.F). J.Z. was supported by a University of Delaware Graduate fellowship. Research in the Martienssen Laboratory is supported by a grant from NIH (RO1GM067014 to R.M.) and by the Howard Hughes Medical Institute and Gordon and Betty Moore Foundation. The authors acknowledge this work was performed with assistance from the Cold Spring Harbor Laboratory Shared Resources, which are funded, in part, by the Cancer Center Support Grant (5PP30CA045508) and declare no competing interests.

References

1. Allen E, Xie Z, Gustafson AM, Carrington JC. microRNA-directed phasing during trans-acting siRNA biogenesis in plants. Cell. 2005; 121:207–221. [PubMed: 15851028]
2. Ronemus M, Vaughn MW, Martienssen RA. MicroRNA-targeted and small interfering RNA-mediated mRNA degradation is regulated by argonaute, dicer, and RNA-dependent RNA polymerase in Arabidopsis. Plant Cell. 2006; 18:1559–1574.10.1105/tpc.106.042127 [PubMed: 16798886]
3. Cuperus JT, et al. Unique functionality of 22-nt miRNAs in triggering RDR6-dependent siRNA biogenesis from target transcripts in Arabidopsis. Nat Struct Mol Biol. 2010; 17:997–1003. [PubMed: 20562854]

4. Law JA, Jacobsen SE. Establishing, maintaining and modifying DNA methylation patterns in plants and animals. Nat Rev Genet. 2010; 11:204–220. rg2719. 10.1038/nrg2719 [PubMed: 20142834]
5. Slotkin RK, et al. Epigenetic Reprogramming and Small RNA Silencing of Transposable Elements in Pollen. Cell. 2009; 136:461–472. [PubMed: 19203581]
6. Tanurdzic M, et al. Epigenomic Consequences of Immortalized Plant Cell Suspension Culture. PLoS Biology. 2008; 6:e302.
7. McCue AD, Nuthikattu S, Reeder SH, Slotkin RK. Gene Expression and Stress Response Mediated by the Epigenetic Regulation of a Transposable Element Small RNA. PLoS Genetics. 2012; 8:e1002474.10.1371/journal.pgen.1002474.t001 [PubMed: 22346759]
8. Nuthikattu S, et al. The Initiation of Epigenetic Silencing of Active Transposable Elements Is Triggered by RDR6 and 21–22 Nucleotide Small Interfering RNAs. PLANT PHYSIOLOGY. 2013; 162:116–131.10.1104/pp.113.216481 [PubMed: 23542151]
9. Mirouze M, et al. Selective epigenetic control of retrotransposition in Arabidopsis. Nature. 2009; 461:427–U130. [PubMed: 19734882]
10. Miura A, et al. Mobilization of transposons by a mutation abolishing full DNA methylation in Arabidopsis. Nature. 2001; 411:212–214. [PubMed: 11346800]
11. German MA, Luo S, Schroth G, Meyers BC, Green PJ. Construction of Parallel Analysis of RNA Ends (PARE) libraries for the study of cleaved miRNA targets and the RNA degradome. Nat Protoc. 2009; 4:356–362. papers2://publication/doi/. 10.1038/nprot.2009.8 [PubMed: 19247285]
12. Hsieh TF, et al. Genome-wide demethylation of Arabidopsis endosperm. Science. 2009; 324:1451–1454. [PubMed: 19520962]
13. Gehring M, et al. DEMETER DNA glycosylase establishes MEDEA polycomb gene self-imprinting by allele-specific demethylation. Cell. 2006; 124:495–506.10.1016/j.cell.2005.12.034 [PubMed: 16469697]
14. Schwab R, Speth C, Laubinger S, Voinnet O. Enhanced microRNA accumulation through stemloop-adjacent introns. EMBO reports. 2013; 14:615–621.10.1038/embor.2013.58 [PubMed: 23661080]
15. Jeong DH, et al. Massive Analysis of Rice Small RNAs: Mechanistic Implications of Regulated MicroRNAs and Variants for Differential Target RNA Cleavage. THE PLANT CELL ONLINE. 2012; 23:4185–4207. papers2://publication/doi/. 10.1105/tpc.111.089045
16. Axtell MJ, Bartel DP. Antiquity of microRNAs and their targets in land plants. The Plant cell. 2005; 17:1658–1673.10.1105/tpc.105.032185 [PubMed: 15849273]
17. Chen HM, et al. 22-Nucleotide RNAs trigger secondary siRNA biogenesis in plants. Proc Natl Acad Sci U S A. 2010; 107:15269–15274. [PubMed: 20643946]
18. Mari-Ordonez A, et al. Reconstructing de novo silencing of an active plant retrotransposon. Nat Genet. 2013; 45:1029–1039.10.1038/ng.2703 [PubMed: 23852169]
19. Wu L, et al. DNA Methylation Mediated by a MicroRNA Pathway. Molecular cell. 2010; 38:465–475. [PubMed: 20381393]
20. Jauvion V, Rivard M, Bouteiller N, Elmayan T, Vaucheret H. RDR2 partially antagonizes the production of RDR6-dependent siRNA in sense transgene-mediated PTGS. PLoS ONE. 2012; 7:e29785. papers2://publication/uuid/722C12F4-2345-4441-A712-569DBA2D0891. [PubMed: 22242179]
21. Slotkin RK, Freeling M, Lisch D. Heritable transposon silencing initiated by a naturally occurring transposon inverted duplication. Nature Genetics. 2005; 37:641–644. papers2://publication/doi. 10.1038/ng1576 [PubMed: 15908951]
22. Stroud H, Greenberg MVC, Feng S, Bernatavichute YV, Jacobsen SE. Comprehensive Analysis of Silencing Mutants Reveals Complex Regulation of the Arabidopsis Methylome. Cell. 2013; 152:352–364. [PubMed: 23313553]
23. Jeddeloh JA, Stokes TL, Richards EJ. Maintenance of genomic methylation requires a SWI2/SNF2-like protein. Nature Genetics. 1999; 22:94–97. [PubMed: 10319870]
24. Teixeira FK, et al. A role for RNAi in the selective correction of DNA methylation defects. Science. 2009; 323:1600–1604. [PubMed: 19179494]
25. Poethig RS. Small RNAs and developmental timing in plants. Current opinion in genetics & development. 2009; 19:374–378. [PubMed: 19703647]

26. Martienssen R, Barkan A, Taylor WC, Freeling M. Somatically heritable switches in the DNA modification of Mu transposable elements monitored with a suppressible mutant in maize. Genes Dev. 1990; 4:331–343. [PubMed: 2159936]
27. Martienssen R, Baron A. Coordinate suppression of mutations caused by Robertson's mutator transposons in maize. Genetics. 1994; 136:1157–1170. [PubMed: 8005422]
28. Poethig RS. Phase change and the regulation of shoot morphogenesis in plants. Science. 1990; 250:923–930.10.1126/science.250.4983.923 [PubMed: 17746915]
29. Wright DA, Voytas DF. Athila4 of Arabidopsis and Calypso of soybean define a lineage of endogenous plant retroviruses. Genome research. 2002; 12:122–131.10.1101/gr.196001 [PubMed: 11779837]
30. Calarco JP, et al. Reprogramming of DNA methylation in pollen guides epigenetic inheritance via small RNA. Cell. 2012; 151:194–205.10.1016/j.cell.2012.09.001 [PubMed: 23000270]
31. Mosher RA, et al. Uniparental expression of PolIV-dependent siRNAs in developing endosperm of Arabidopsis. Nature. 2009; 460:283–286. [PubMed: 19494814]
32. Bagijn MP, et al. Function, targets, and evolution of Caenorhabditis elegans piRNAs. Science (New York, NY). 2012; 337:574–578. papers2://publication/doi/. 10.1126/science.1220952
33. Shirayama M, et al. piRNAs initiate an epigenetic memory of nonself RNA in the C. elegans germline. Cell. 2012; 150:65–77. papers2://publication/doi/. 10.1016/j.cell.2012.06.015 [PubMed: 22738726]
34. Regulski M, et al. The maize methylome influences mRNA splice sites and reveals widespread paramutation-like switches guided by small RNA. Genome Res. 2013; 23:1651–1662.10.1101/gr.153510.112 [PubMed: 23739895]
35. Krueger F, Andrews SR. Bismark: a flexible aligner and methylation caller for Bisulfite-Seq applications. Bioinformatics. 2011; 27:1571–1572.10.1093/bioinformatics/btr167 [PubMed: 21493656]
36. Zhai J, et al. MicroRNAs as master regulators of the plant NB-LRR defense gene family via the production of phased, trans-acting siRNAs. Genes & Development. 2011; 25:2540–2553.10.1101/gad.177527.111 [PubMed: 22156213]

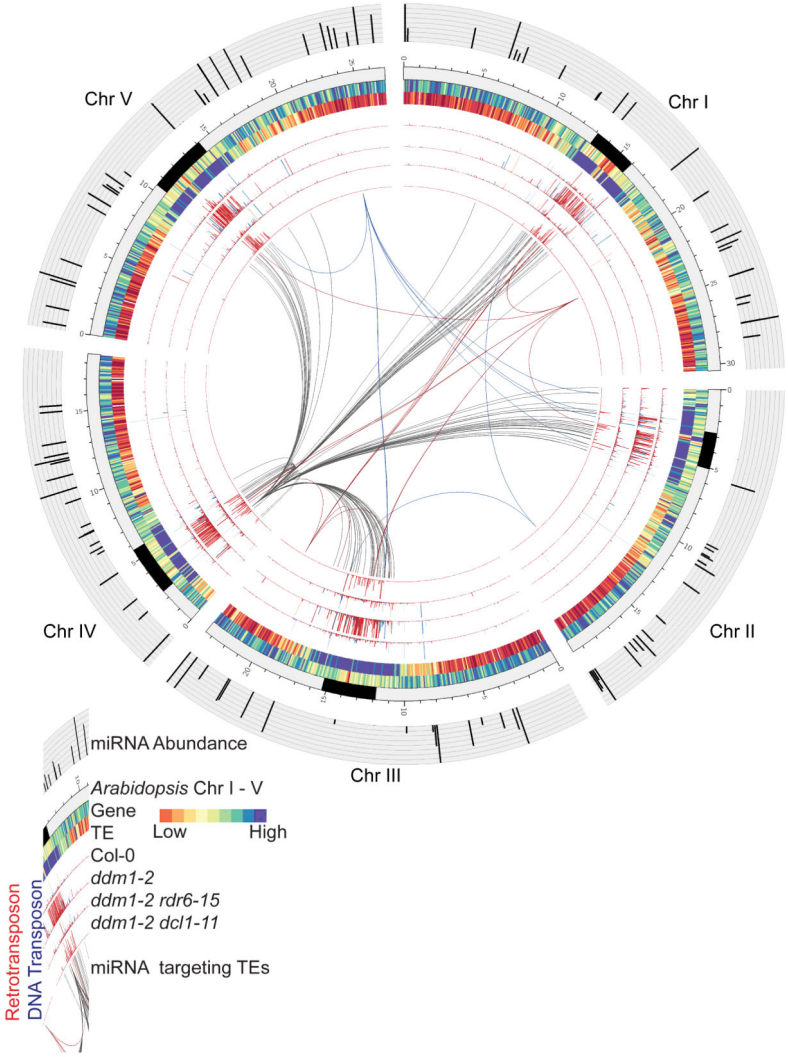

Figure 1. miRNAs trigger *RDR6*-dependent 21-nt epigenetically activated (ea)siRNA biogenesis from reactivated transposons

Whole-genome representation illustrating miRNAs triggering widespread easiRNA biogenesis at transposons in *Arabidopsis*. Outermost to innermost tracks depicting: miRNA abundance in *ddm1-2* (Histogram); *Arabidopsis* Chromosome I – V, pericentromeric region (black) (Ideogram); Gene and transposon frequency, low density (red), high density (blue) (Heat-map); Retrotransposon derived 21-nt sRNAs (dark red = unique, light red = multiple mapping) and DNA transposon-derived 21-nt sRNAs (dark blue = unique, light blue = multiple mapping) 21-nt siRNAs in order of Col-0, *ddm1-2*, *ddm1-2 rdr6-15*, and *ddm1-2 dcl1-11* (Histogram); miRNAs targeting transposons (Connectors); miR859a (Chr I, red), miR390a (Chr II, blue), miR172d (Chr III, red), eamiR2 *ATHILAIV* (Chr IV, grey) and miR172e (Chr V, blue). Transposons are post-transcriptionally targeted by 50 known miRNAs and newly discovered eamiRNAs (Table 1) giving rise to abundant *RDR6*-dependent 21-nt easiRNAs at transposons in *Arabidopsis.* (Refer to Extended Data Fig. 1; Supplementary Table 1; 3).

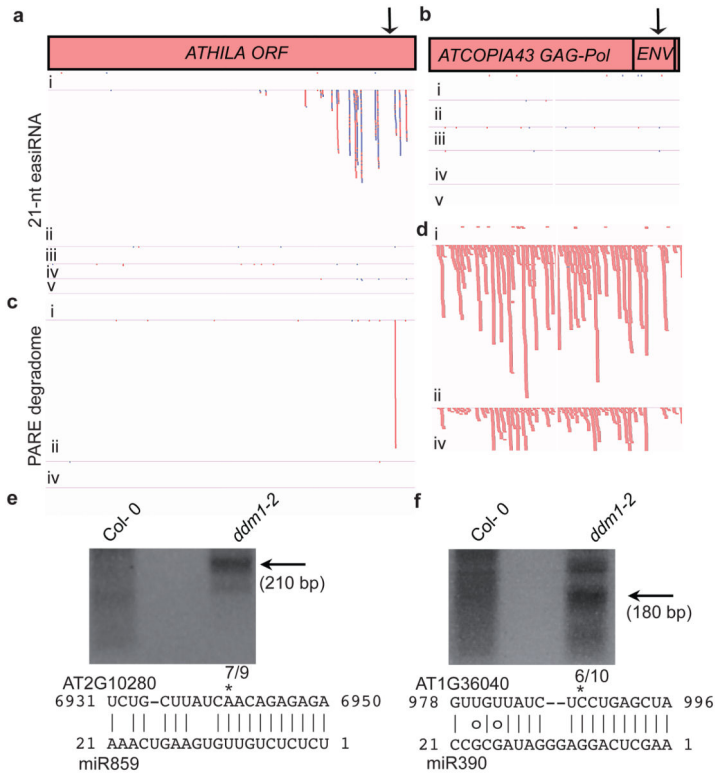

Figure 2. miRNA cleavage at *ATHILA ORF1* and *ATCOPIA43*

(a, b) 21-nt easiRNAs at *ATHILA ORF1* (AT2G10280), in comparison to non-easiRNA generating *ATCOPIA43* (AT1G36040) in track order Col-0 (i), *ddm1-2* (ii), *rdr6-15* (iii), *ddm1-2 rdr6-15* (iv) and *ddm1-2 dcl1-11* (v). (c, d) Parallel Analysis of RNA Ends (PARE) at *ATHILA ORF1* and *ATCOPIA43 in* track order Col-0 (i), *ddm1-2* (ii) and *ddm1-2 rdr6-15* (iv). Individual reads, sense = red, antisense = blue. (e, f) 5′ RLM RACE-PCR products (arrows; black bars in a, b) from *ATHILA ORF1* and *ATCOPIA43* corresponding to cleaved mRNA fractionated by gel electrophoresis. Inset: miRNA alignment with 5′ RLM RACE-PCR cleavage sites, and frequencies of cleavage products indicated as fractions.

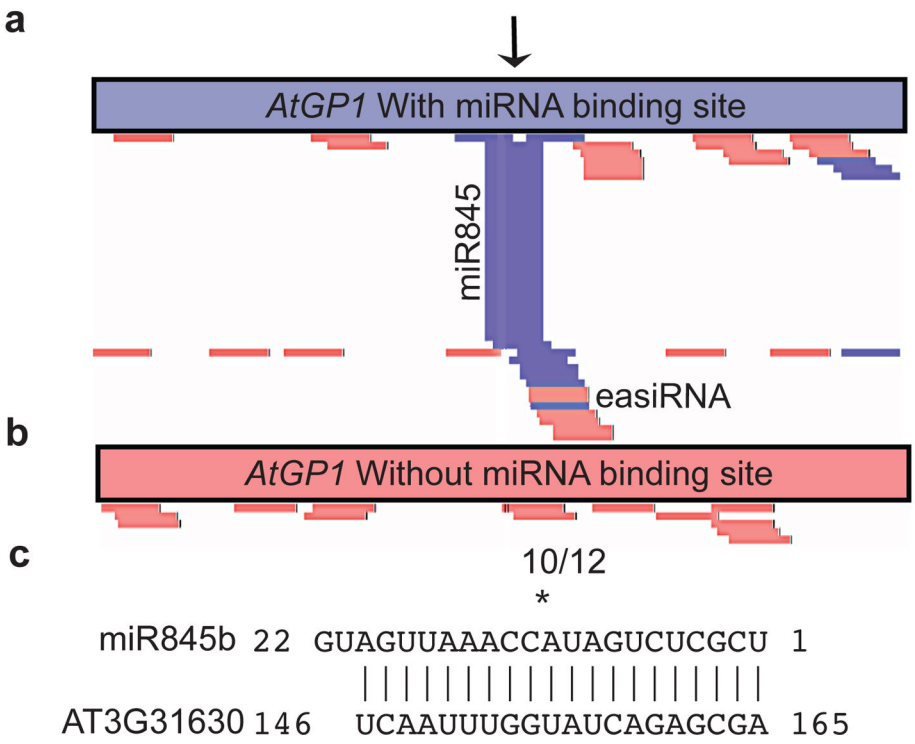

Figure 3. miR845b targets *AtGP1* promoting easiRNA biogenesis

(a) Transgenic line over-expressing *AtGP1* containing the 20-nt miR845b target region (marked miR845) and novel overlapping 21-nt easiRNAs (star). Individual reads, sense = red, antisense = blue. (b) Transgenic line over-expressing *AtGP1* that did not contain the 20-nt miR845b predicted target region, with no 21-nt easiRNAs overlapping this site. (c) Frequencies of 5′ RLM RACE-PCR miR845b *AtGP1* cleavage products indicated as fractions.

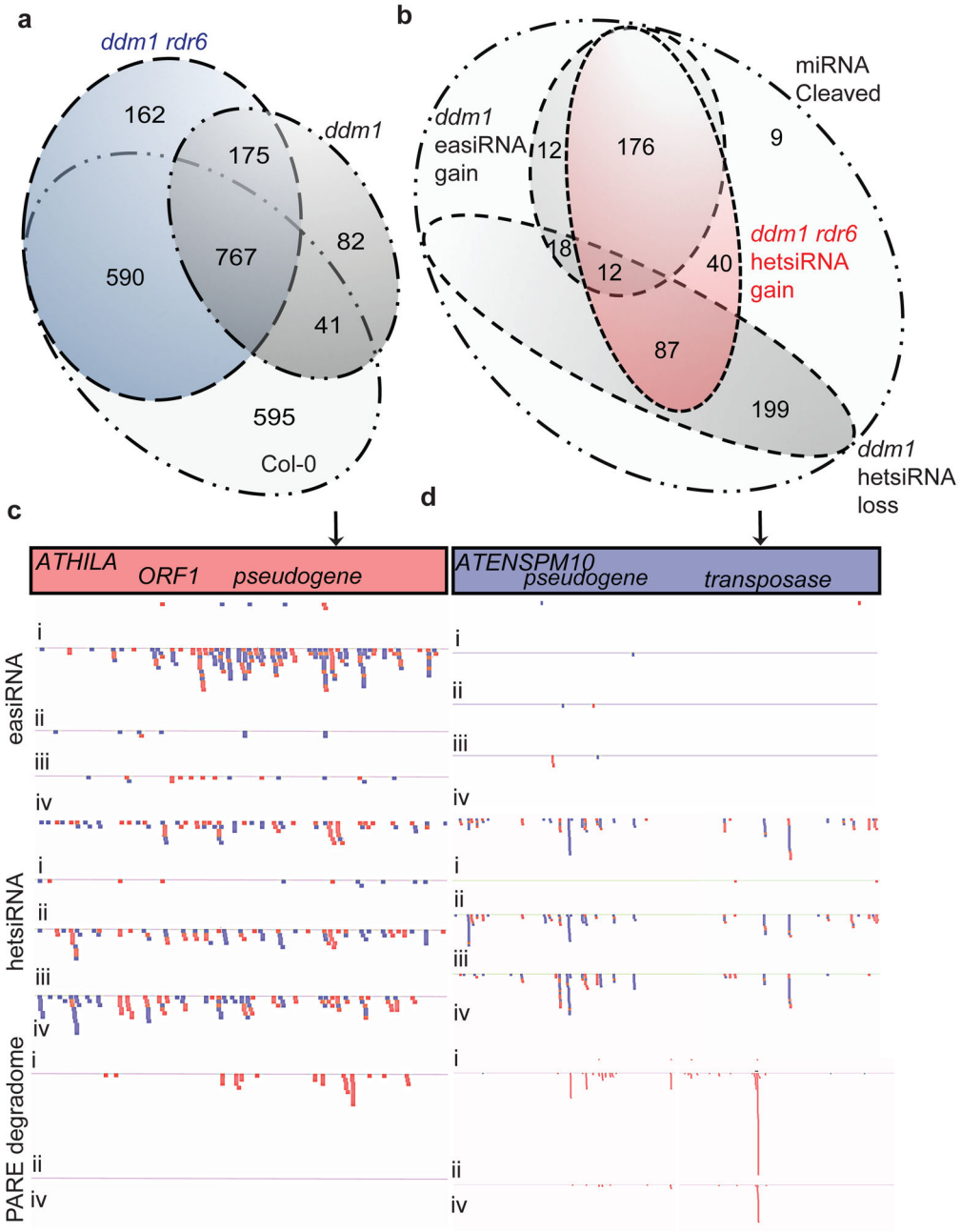

Figure 4. Transposons targeted by miRNA, gain hetsiRNA when the easiRNA pathway is lost

(a) Overlap of transposons targeted by hetsiRNAs in Col-0, *ddm1-2* and *ddm1-2 rdr6-15*. (b) Overlap of transposons targeted by miRNAs, that have lost hetsiRNAs in *ddm1-2*, gained hetsiRNAs in *ddm1-2 rdr6-15*, and those whose transcripts undergo productive miRNA cleavage resulting in easiRNA biogenesis in *ddm1-2*. 21-nt easiRNAs, 24-nt hetsiRNAs and PARE degradome at easiRNA-generating (c) *ATHILA* (AT3G32118) in comparison to non-easiRNA generating (d) *ATENSPM1* (AT4G02314). Individual reads, sense = red, antisense = blue in track order Col-0 (i), *ddm1-2* (ii) *rdr6-15* (iii), and *ddm1-2 rdr6-15* (iv).

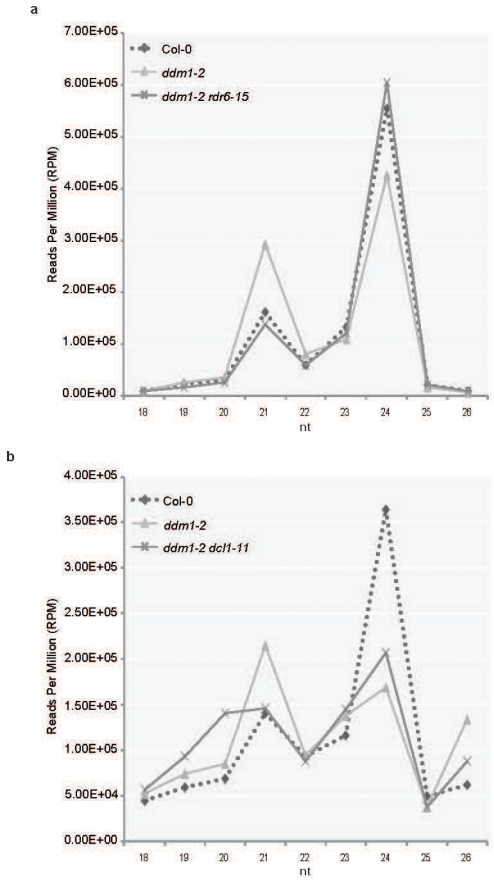

Extended Data Figure 1. 21-nt easiRNAs originate from transposons in *ddm1* and are miRNA and *RDR6*-dependent

(a) 18-nt to 26-nt small RNA abundance in Col-0, *ddm1-2*, and *ddm1-2 rdr6-15*. Normalized reads per million (RPM). (b) 18-nt to 26-nt small RNA abundance in Col-0, *ddm1-2*, and *ddm1-2 dcl1-11*. Normalized reads per million (RPM).

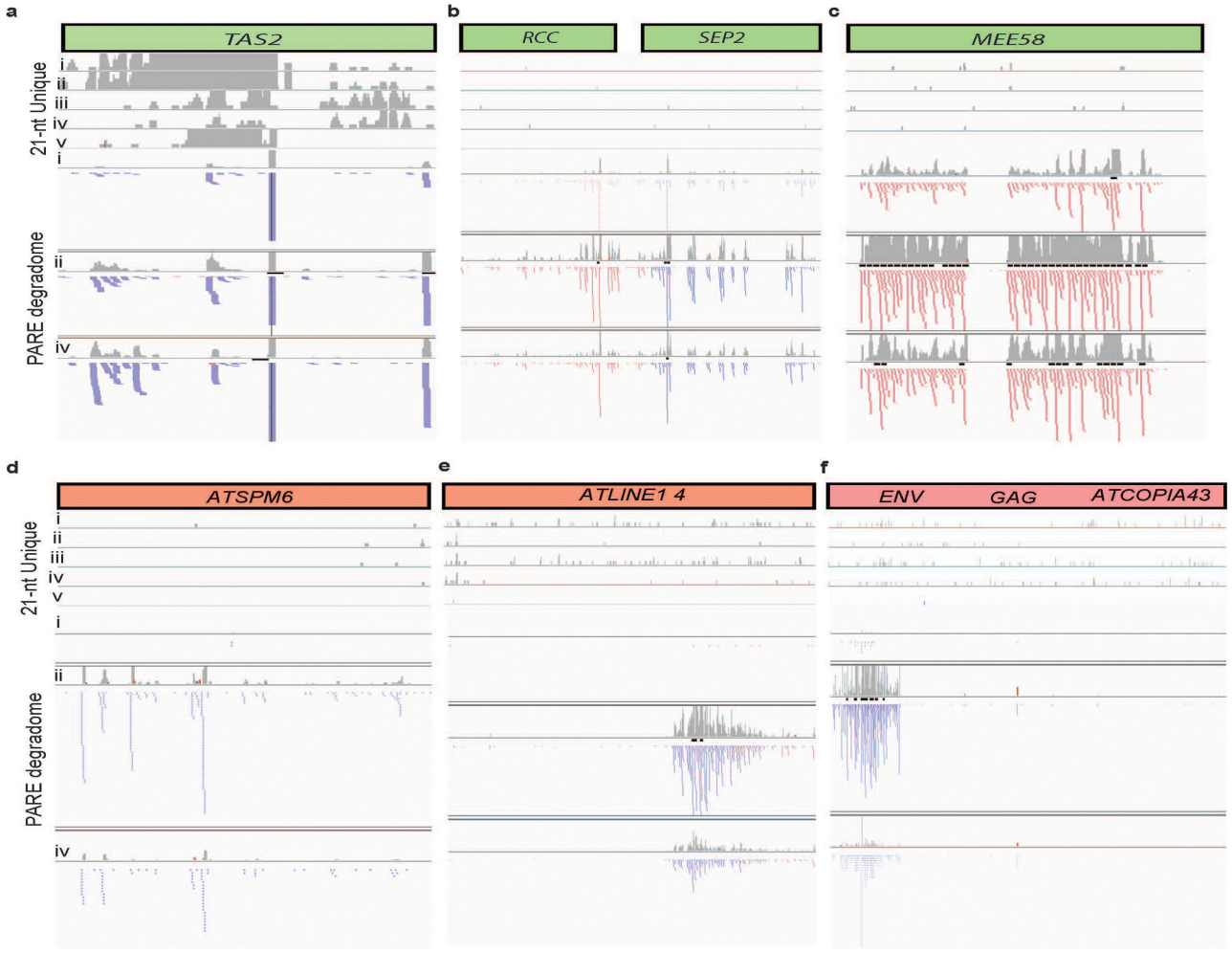

Extended Data Figure 2. miRNA target genes and transposons that do not promote tasiRNA nor easiRNA, respectively, have degradation covering the entire region

Read pattern distribution of 21-nt unique reads (represented as a histogram of read density (grey bars)) and PARE signatures at (a) *TAS2* (AT2G39681), (b) *RCC* (AT3G02300), *SEP2* (AT3G02310), (c) *MEE58* (AT4G13940), and transposons (d) *ATENSPM6 (*AT2G06720), (e) *ATLINE1_4 (*AT2G15540), (f) *ATCOPIA43 (*AT3G0410), in track order Col-0, *ddm1-2*, *rdr6-15*, *ddm1-2 rdr6-15* and *ddm1-2 dcl1-11*.

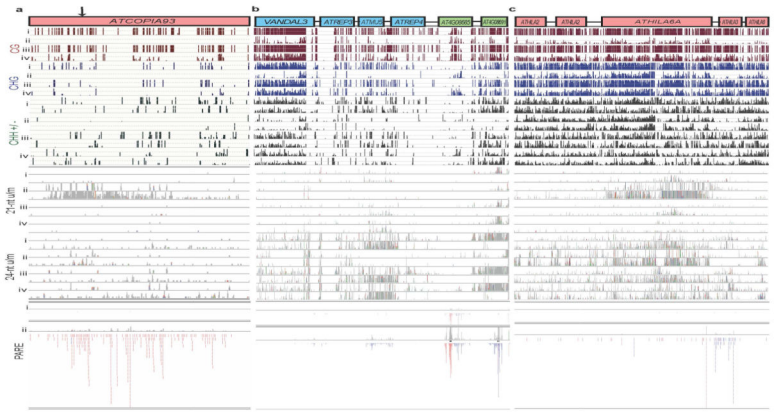

Extended Data Figure 3. Relationship between DNA methylation, easiRNA and hetsiRNA at transposons that miRNA are predicted to target

DNA methylation, by CG (red), CHG (blue) and CHH+/− context (green) cytosine context (scale 1 = methylated cytosine, 0 = unmethylated cytosine) at (a) *ATCOPIA93* (AT5G17125), (b) *ATMU5* (AT4G08680) DNA transposon and the surrounding region, and (c) *ATHILA6A* (AT4TE15030) retrotransposon and the surrounding region, in Col-0, *ddm1-2*, *rdr6-15* and *ddm1-2 rdr6-15* (i). 21-nt and 24-nt siRNAs, represented as a histogram of read density (grey bars) in track order Col-0, *ddm1-2*, *rdr6-15* and *ddm1-2 rdr6-15* (ii). Key for sRNA reads, unique (U) mapping to one location of the genome, and multiple (M) mapping to more than one location of the genome. PARE read density in Col-0 and *ddm1-2* (iii).

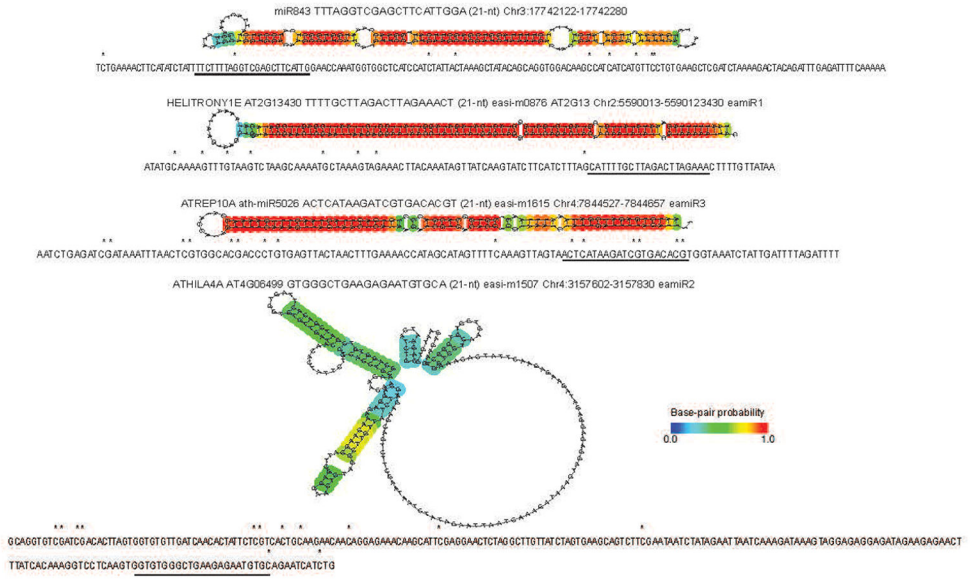

Extended Data Figure 4. Epigenetically activated (ea)miRNA immature precursor sequence and predicted structure

Epigenetically activated (ea)miRNAs immature precursor sequences have methylated cytosines (*) in Col-0, that are unmethylated in *ddm1-2*. Mature miRNA are underlined, and the putative stem-loop structures of the precursors are illustrated.

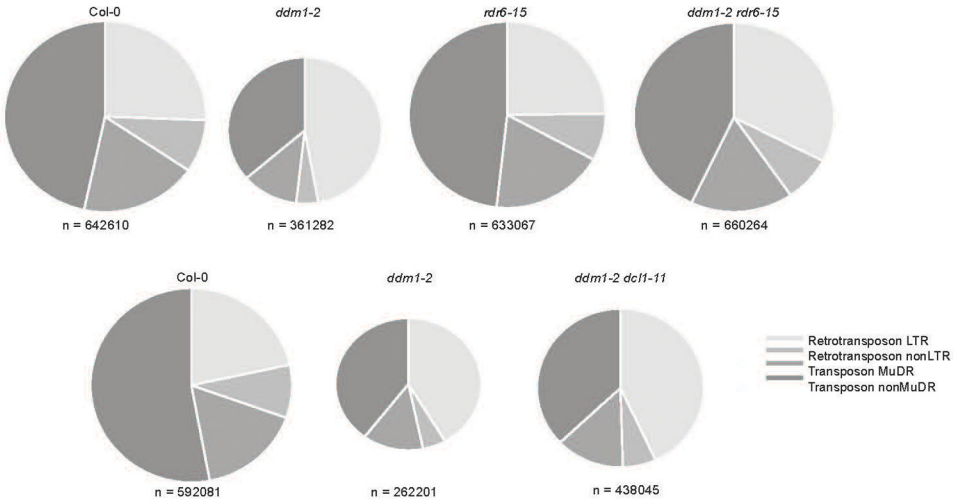

Extended Data Figure 5. 24-nt hetsiRNAs at transposons in Col-0, are lost in *ddm1*, and gained in *ddm1 rdr6* and *ddm1 dcl1*

24-nt hetsiRNAs by transposon class in Col-0, *ddm1-2*, *rdr6-15*, *ddm1-2 rdr6-15*, and *ddm1-2 dcl1-11*. Normalized reads per million (RPM).

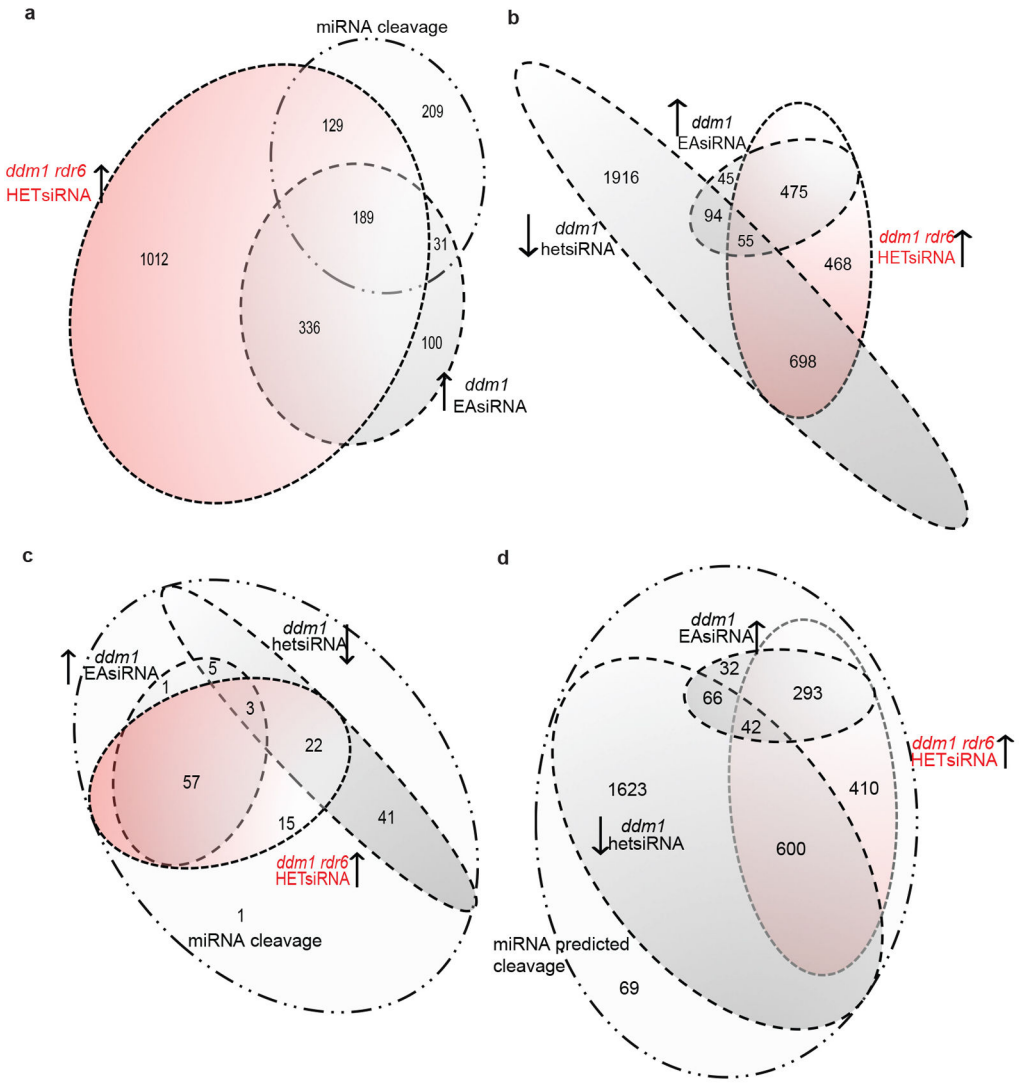

Extended Data Figure 6. Overlap of TEs that undergo easiRNA biogenesis, hetsiRNA loss and miRNAs targeting

Individual transposons were grouped depending on small RNA abundance in each genotype. (a) TEs that lose 24-nt hetsiRNAs in *ddm1-2*, gain 21-nt easiRNAs in *ddm1-2* overlap with those that gain 24-nt hetsiRNAs in *ddm1-2 rdr6-15*. (b) TEs that are targeted and cleaved by miRNAs overlap with those that gain 21-nt easiRNAs in *ddm1-2* and 24-nt hetsiRNAs in *ddm1-2 rdr6-15*. (c) TEs that are targeted and cleaved by two or more miRNAs overlap with those that gain 21-nt easiRNAs in *ddm1-2*, and those that gain 24-nt hetsiRNAs in *ddm1-5 rdr6-15*. (d) TEs that are predicted to be targeted by miRNAs, but without supporting PARE cleavage data, also overlap with those that gain 21-nt easiRNAs in *ddm1-2* and 24-nt hetsiRNAs in *ddm1-2 rdr6-15*.

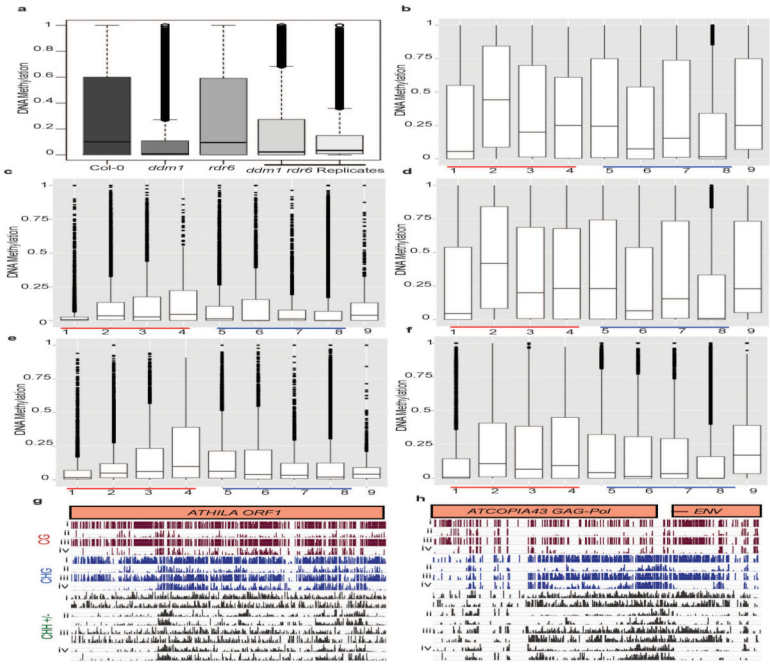

Extended Data Figure 7. Loss of methylation at transposons in *ddm1* is partially restored in *ddm1 rdr6*

(a) Transposon methylation in Col-0, *ddm1-2*, *rdr6-15* and *ddm1-2 rdr6-15* replicates. Scale 1 = methylated cytosine, 0 = unmethylated cytosine. Total DNA methylation at transposons, grouped by superfamily in (b) Col-0, (c) *ddm1-2*, (d) *rdr6-15* and (e, f) *ddm1-2 rdr6-15* replicates. Key (1) LTR Retrotransposons *ATGYPSY*, (2) LTR Retrotransposons *ATCOPIA*, (3) NonLTR Retrotransposons *ATLINE*, (4) nonLTR Retrotransposons *TSCL*, (5) TIR DNA Transposons MuDR, (6) non-TIR DNA Transposons MuDR, (7) DNA Transposons *EnSpM*, (8) DNA Transposons *Helitron* and (9) Other Repeats. Total methylation by total converted cytosine to thymine and non-converted cytosine counts (at least 10 reads per cytosine). Scale 0 = unmethylated, 1 = methylated. Boxplots indicate median, range and standard deviations (box). DNA methylation, by CG (red), CHG (blue) and CHH+/− context (Green) at (g) *ATHILA* ORF1 (AT2G10280) and (h) *ATCOPIA43* (AT1G36040). Track order Col-0 (i), *ddm1-2* (ii), *rdr6-15* (iii) and *ddm1-2 rdr6-15* (iv).

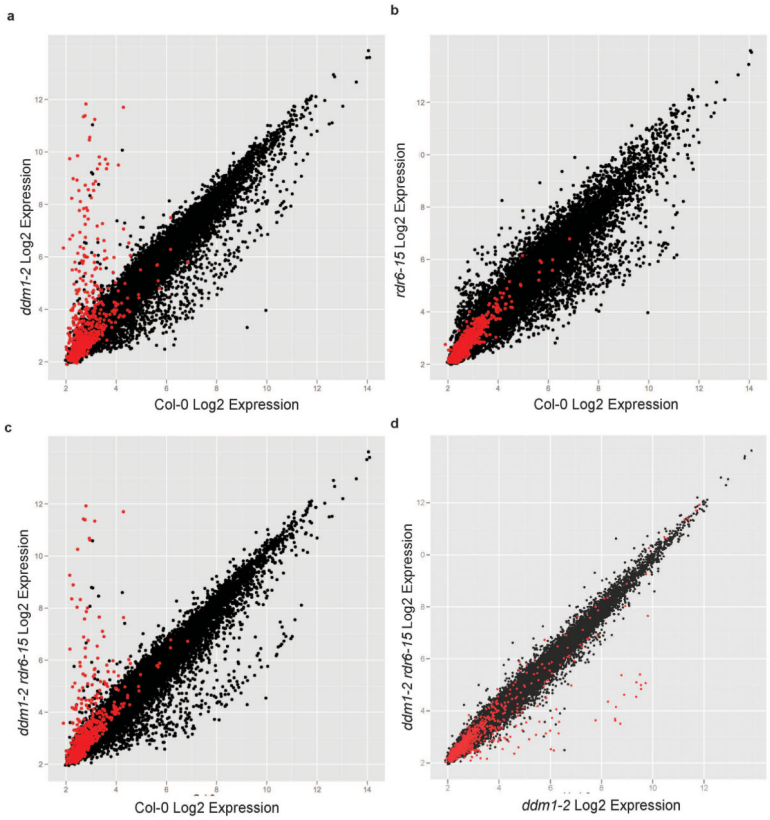

Extended Data Figure 8. Transposon transcript abundance in *ddm1-2* and *ddm1 rdr6*

(a, b, c) *Ath1* Affymetrix microarray expression (log2 signal intensity) in Col-0 in comparison to *ddm1-2*, *rdr6-15* and *ddm1-2 rdr6-15*. (d) TEs upregulated in *ddm1-2* were not further upregulated in *ddm1-2 rdr6-15*. Key: red = transposons, black = genes.

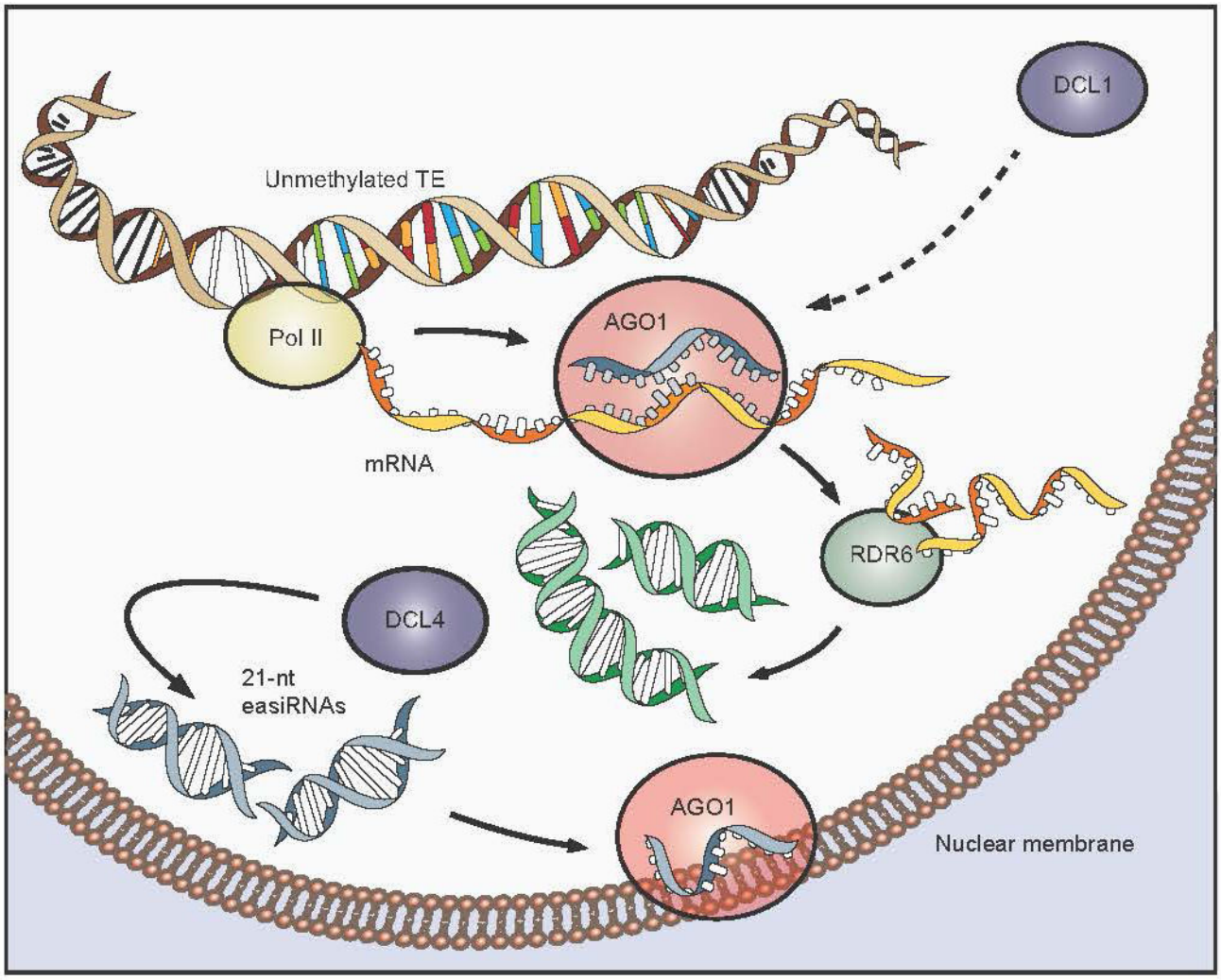

Extended Data Figure 9. miRNA-directed easiRNA biogenesis from activated transposons

When TEs are epigenetically activated, through the loss of DNA methylation and/or heterochromatin, transposon mRNA transcripts become preferentially targeted by miRNAs (*DCL1*-dependent) bound by AGO1. Productive cleavage of transposon transcripts engages RDR6 and DCL4, which generate 21-nt epigenetically-activated (ea)siRNAs from transposon open reading frames, in a post-transcriptional gene silencing (PTGS) mechanism, that are then loaded into AGO1, and thus, prevents engagement of RDR2 and RdDM. This antagonism accounts for the retention of miRNA binding sites by transposons, to evade long-term heritable silencing, elicited by DNA methylation via *RDR2*. This model also accounts for the retention of the miRNA-directed mechanism by the host organism, in order to generate easiRNAs to silence TEs when they are epigenetically reprogrammed in the germline.

Ath miRNA (nt)	TRANSPOSON TARGETS
miR156 (20)	***ATNSPM5**** , *ATNSPM6**
miR157a (21)	***ATHILA4**** , *ATHILA4*, ***ATNSPM5**** , *ATNSPM6*,
miR159 (21)	***ATGP3**** , ***ATGP7**** , *ATLINE1_4**
miR162 (21)	*VANDAL6*
miR167 (21, 22)	***ATHILA2**** , ***ATHILA2***, ATLINE1_5, *ATLINE1_4*
miR169 (21)	*ATLANTYS*, ATLINE1A,
miR172b-star (20)	ATCOPIA43, *ATGP7*, ARNOLD1, ARNOLD2, *ARNOLD3**, ARNOLD4
miR2111 (21)	***ATHILA2**** , ***ATHILA2, ATHILA3**** , **ATHILA4C**, **ATHILA6A, ATHILA6B, VANDAL7***
miR319 (21)	**ATGP7***, ***ATGP3**** ,
miR390 (21)	ATCOPIA9, ATCOPIA22, ATCOPIA43, ATCOPIA89, ATHILA8B
miR395 (21)	**ATHILA2, *ATHILA3**** , **ATHILA6A***, VANDAI21
miR396 (21)	ATCOPIA49, ATCOPIA66, *VANDAL21*, ***ATNSPM6,* ATIS112A,** ATNSPM5
miR399 (21)	**ATHILA2***, ARNOLD2, *ARNOLD2**, ARNOLD4, ARNOLD3, ATLINE1_6, **ATLANTYS1**
miR415 (21)	**ATCOPIA95*, ATHILA2*, ATHILA4, ATHILA6A, ATHILA6B,** ATSPM5, ATNSPM6, *VANDAL3*, ***VANDAL3,*** ATHILA2
miR418 (21)	***ATHILA2***
miR420 (21)	**ATHILA6A**
miR447 (22)	ATCOPIA51, ***ATHILA3**** , ***ATHILA****
mR447a2 (21)	ATHILA, ATHILA3
miR5015 (21)	**ATCOPIA48,** ATCOPIA80, VANDAL3
miR5020 (21)	ATNSPM1
miR5022 (21)	**ATHILA2*, ATHAT3*,** ATSPM1A
miR5029 (21)	*ATNSPM5*
miR771 (22)	***ATHILA2****
miR774 (21)	**ATHILA ORF1***, ***ATHILA**** , *ATHILA*, HELITRON3, VANDAL4, ***VANDAL4****
miR775 (20)	***ATHILA2**** , ***ATHILA2***
miR780 (21)	***ATHILA2**** , *ATHILA2*, ATCOPIA89, VANDAL4
miR823 (21)	***ATGP2**** , ATHILA4C, **ATHILA3***
miR825 (21)	ATNSPM5, *ATNSPM10**
miR833 (22)	***ATHILA3**** , **ATHILA6**
miR834 (21)	**ATCOPIA61**
miR838 (21)	ARNOLD1, *ARNOLD2**, *VANDAL3**, ATLANTYS, ATNSPM5
miR843 (21)	*ATNSPM7*
miR845a (21)	***ATNSPM5***
miR847 (21)	ATHILA4B, ATNSPM9, ATHILA0
miR854a (21)	VANDAL2, VANDAL17, ATHILA4C
miR855 (22)	***ATHILA6A,*** ATHILA3
miR858 (21)	VANDAL3
miR859 (21)	***ATHILA**** , **ATHILA ORF1*** , ***ATHIIA6A,* ATNSPM10***
miR861 (21)	**ATHILA ORF1***, ***ATHILA****
miR862 (21)	***ATHILA2,*** *VANDAL1*
miR863 (21)	**ATNSPM9,** ARNOLD3,
miR866 (21)	**ATGP2,** *VANDAL8*
miR869 (21)	*ATNSPM1A**
Ath eamiRNA (nt)	
(ea)miR843 (21)	**TA11,** ATHILA4A, *ATNSPM7*, STLINE1_6
(ea)miR172c (22)	ATCOPIA43, *ATLANTYS1**, **ATHILA6B, ATNSPM10,** ATCOPIA81, ATCOPIA89,
eamiR1 (21)	ATNSPM2, **ATHILA6A, *ATHILA2,* ATLINE1_6, ATGP10*, ATHILA4C*, VANDAL2, ATCOPIA95, ATHILA2, ATLANTYS3,** *ATHILA4,*
eamiR2 (21)	***ATHILA4**** , *ATLANTYS2, ATLANTYS1*,
eamiR3 (21)	ATCOPIA43

Extended Data Figure 10. *Arabidopsis* miRNAs target transposons

Known *Arabidopsis* miRNAs, and novel epigenetically-activated (ea)miRNAs that arise in *ddm1-2*, are predicted to target transposon transcripts and confirmed to cleave transposon transcripts by PARE (Supplementary Table 3; Supplementary Methods). eamiRNAs, some known to be developmentally regulated, and TE-derived eamiRNAs that target specific transposon families. Transposons are identified by EVRY TE identifier (Supplementary Table 2, for further annotation refer to The *Arabidopsis* Information (TAIR10) annotation ORF ID). Transposon transcripts giving rise to 21-nt easiRNAs (**bold**); those that are targeted by multiple miRNA (*); and, those miRNAs that target multiple transposons of the same family (*italics*) are highlighted.